Using iterated rational filter banks within the ARSIS concept for producing 10 m Landsat multispectral images

Philippe Blanc, Thierry Blu, Thierry Ranchin, Lucien Wald, Roberto Aloisi

Blanc Ph., Blu T., Ranchin T., Wald L., Aloisi R., 1998. Using iterated rational filter banks within the ARSIS concept for producing 10 m Landsat multispectral images. International Journal of Remote Sensing, 19, 12, 2331-2343.

Using iterated rational filter banks within the ARSIS concept for producing 10 m Landsat multispectral images.

Philippe Blanc[1,2] - Thierry Blu[3] - Thierry Ranchin[1] - Lucien Wald[1] - Roberto Aloisi[2]

1 - Groupe Télédétection & Modélisation, Centre d'Energétique, Ecole des Mines de Paris.
Rue Claude Daunesse, B.P. 207, F-06904 Sophia Antipolis cedex, France.

2 - Service performances et applications de l'imagerie. SE/TNA Aérospatiale.
B.P. 99, 06322 Cannes la Bocca, France.

3 - France Telecom, CNET PAB/STC.
Rue du général Leclerc, F-92191 Issy-les-Moulineaux, France.

Corresponding author: Wald Lucien
Tel. (33) 04 93-95-74-49 Fax (33) 04 93-95-75-35 Email wald@cenerg.cma.fr

Running title: Producing 10 m Landsat multispectral images

Abstract: The ARSIS concept is meant to increase the spatial resolution of an image without modification of its spectral contents by merging structures extracted from a higher resolution image of the same scene but in a different spectral band. It makes use of wavelet transforms and multiresolution analysis. It is currently applied in an operational way with dyadic wavelet transforms that limit the merging of images whose ratio of their resolution is a power of two. Nevertheless, provided some conditions, rational discrete wavelet transforms can be numerically approximated by rational filter banks which would enable a more general merging: indeed, in theory, the ratio of the resolution of the images to merge is a power of a certain family of rational numbers. The aim of this article is to examine whether the use of those approximations of rational wavelet transforms are efficient within the ARSIS concept.

This work relies on a particular case: the merging of a 10 m SPOT Panchromatic image and a 30 m Landsat Thematic Mapper multispectral image to synthesize 10 m multispectral image called TM-HR.

1. INTRODUCTION

Many thematic applications using remotely sensed multispectral images come up against the limit of their relatively low spatial resolution. The ARSIS concept, French acronym for "Amelioration de la Résolution Spatiale par Injection de Structures", provides a solution to this issue (Mangolini *et al.* 1992, 1993). Indeed, the original principle of the ARSIS concept is to merge two images, one having interesting spectral characteristics, the other a better spatial resolution. The result image combines both properties, *i.e.* the best resolution without altering the spectral contents of the image. More precisely, thanks to multiresolution analysis provided by wavelet transform, the ARSIS concept enables to increase the spatial resolution of an image without modification of its spectral content by merging structures extracted from a higher resolution image of the same scene.

Nowadays, this concept is operationally applied with dyadic wavelet transforms (*i.e.* ratio of resolution is 1/2). For example, it has been put into practice on SPOT data. The image products corresponding to each 20 m resolution spectral channel of SPOT - XS_1, XS_2, and XS_3 are merged with the 10 m Panchromatic image to synthesize a 10 m resolution for each channel called XS-HR. For more information about the ARSIS concept and its operational application on SPOT data, see Ranchin *et al.* (1993).

However, the use of dyadic wavelet transform within the ARSIS concept limits the merging of images with a resolution ratio equal to a power of two (for example, SPOT P and XS, Landsat TM and TM_6, SPOT P, XS and Landsat MSS, SPOT 4 B2 and B1-B3-MIR, SPOT 5, *etc.*). Very good results were also attained in cases where this ratio is close to a power of two, as for instance KVR-1000 and SPOT P or XS (Ranchin, Wald 1996). In order to enable this general concept of merging to be put into application in a more general case, it could be interesting to use non dyadic wavelet transform within a multiresolution analysis. Blu (1993-a-b) proposes a method to synthesize rational filter banks that,

under some conditions, provide an approximation of certain rational wavelet transforms. Those rational filter banks could enable a more general merging than dyadic wavelet transform: indeed, in theory, the ratio of the resolution of the images to merge is a power of a certain family of rational number. But we will see later that there is a limitation on the choice of this rational number.

Therefore, this article presents the study of the use of those filter banks as an approximation of rational wavelet transform within the ARSIS concept. This work relies on a particular case: the merging of a 10 m SPOT Panchromatic image and a 30 m Landsat Thematic Mapper (TM) multispectral image in order to synthesize 10 m multispectral image called TM-HR.

After a description of the study area and the corresponding data from SPOT and Landsat, a short overview is made on rational filter banks and their link with rational wavelet transforms. Then, to assess the efficiency of those filter banks applied in ARSIS, we present an example of merging of a 10 m SPOT Panchromatic image and a 30 m Landsat TM multispectral image. Two approaches were conducted which both used a 2/3 filter bank in ARSIS. Then these two approaches were compared to other approaches that made use of a bicubic interpolation with resampling rate of either 2/3 or 3/2, combined with a dyadic wavelet transform within ARSIS. The study of this particular case will enable us to draw some conclusions on the usefulness of rational filter banks within the ARSIS concept.

2. THE STUDY AREA

The study area for the SPOT-Landsat merging is located in the southeast of France, close to Marseille (France). It is composed of small cities: Berre l'Etang, Rognac, Vitrolles and La Fare les Oliviers, and of rural landscape. The scene is approximately located between 5°05' and 5°15' E in longitude and 43°27' and 43°33' N in latitude and the total area is about 235 sq. km. The rural land in the left hand of the scene is mainly composed by agricultural production (vine). The land extremity into the pond of Berre is a salt marsh. Forest, brushwood and salt marshes are other land-cover types found in the rural area.

3. DATA DESCRIPTION AND DATA PREPROCESSING

A Landsat TM multispectral image (spectral bands TM_1, TM_2, TM_3, TM_4 and TM_5) at 30 m spatial resolution dated 19 August 1991 and a SPOT Panchromatic image at 10 m resolution dated 21 November 1992 are used to synthesize a multispectral image corresponding to the five bands (TM_1, ..., TM_5) at 10 m resolution called hereafter TM-HR. The Landsat TM_1 image is displayed in Figure 1. Figure 2 illustrates the five different spectral bands chosen in Landsat TM and SPOT Panchromatic used for the merging.

The ARSIS concept consists in a merging « pixel to pixel » of the SPOT Panchromatic and the Landsat TM images. Therefore those images have to be superimposed. In order to keep the high frequencies of the Panchromatic image, the Landsat TM images have been resampled using bicubic interpolation. In other words, the SPOT image is subsampled at the resolution of the Landsat images and is the reference for the geometric registration. Nineteen control points have been visually pointed out and a polynomial distortion model was then computed and applied to the multispectral image. The root mean square errors are about 0.37 pixel in the X-direction and 0.31 pixel in the Y-direction.

4. RATIONAL FILTER BANKS AND WAVELET TRANSFORMS

The purpose of this section is to present a short overview of the rational filter banks structure and their link with discrete wavelet transforms. Blu (1993-a) showed that, under some conditions, two-band iterated filter banks with rational rate change p/q can be used to approximate very closely samples of discrete wavelet transform with the same rational dilation factor. More precisely, the structure of rational filter banks is similar to the dyadic filter banks which provide wavelet analysis of the input signal: this general structure is shown in Figure 3. Those filter banks are composed of an iterated low-pass branch and a high-pass branch between two consecutive low-pass branches. The description of the design procedure of the rational lossless finite impulse response (F.I.R.) low-pass and high-pass filters is given in Blu (1993-b).

The dyadic case is obtained with p=1 and q=2. In this case, the high-pass branch outputs are samples of discrete dyadic wavelet transform. In the rational case, this is no longer true. It still could be seen as a kind of multiresolution analysis but the decomposition of the signal is not plainly made on dilated and shifted versions of a single function (the wavelet). Nevertheless, when p=q-1, Blu (1993-a) proved that the difference between the high-pass outputs and the samples of a corresponding rational discrete wavelet transform can be reduced by the selection of suitable parameters in the filters design, so that the iterated rational filter bank can generate a good approximation of a wavelet transform.

As a conclusion, we presently have an approximation of a discrete wavelet transform with a rational dilation factor (q-1)/q at our disposal. The extension of the use of those iterated rational filter banks to image processing is easily done following (Mallat 1989).

For example, when p=2 and q=3, the rational filter bank described by Blu provides an approximation of 2/3 wavelet transform. At each step of the 2/3 wavelet transform, that is to say at each scale, a context image whose resolution is equal to the resolution of the previous context image multiplied by 3/2 is calculated as well as three sets of wavelet coefficients describing the geometric structures in three directions: vertical, horizontal and diagonal. Such a representation of the information in remote sensing has been discussed (Ranchin and Wald 1993). Figure 4 illustrates one iteration of the 2/3 wavelet transform.

We have to notice that the suitable parameters for a good approximation of the wavelet transform lead to a number of coefficients of the filters much greater than in the dyadic case. The low-pass and the high-pass filters to be applied have impulsional responses having respectively 21 and 11 coefficients, which correspond to a width of respectively 21 and 11 pixels.

5. COMPUTING THE TM-HR

Our aim is to synthesize a 10 m multispectral TM-HR image corresponding to the spectral bands TM_1, ..., TM_5 from the merging of a 10 m SPOT Panchromatic image and a 30 m Landsat TM multispectral image of the same geographical area. The ratio of their resolution is 1/3. It is the reason why ARSIS with dyadic wavelet transform cannot be applied in this case. Moreover, we assume, for

the synthesis of a filter bank with a rational rate change p/q, that p=q-1. In other words, the 1/3 wavelet transform cannot be approximated by a rational filter bank. Therefore, two ways exist to synthesize the TM-HR multispectral image with ARSIS. In one way, the 2/3 filter bank can be used, in the other, it is replaced by a bicubic interpolation. For each way, because $1/3 = 1/2 \times 2/3$ or $1/3 = 2/3 \times 1/2$, two possibilities exist : either the dyadic wavelet transform is applied first or last.

The first way consists in using ARSIS with a 2/3 filter bank. Within the first way, there are two possible approaches:

- ***ARSIS$_{1/3}$ #1:*** in this case, the 30 m Landsat TM image is enhanced to 15 m by the use of ARSIS concept applied with a dyadic wavelet transform and the SPOT Panchromatic resampled at the resolution 15 m. Then the 10 m TM-HR image is synthesized from the 10 m SPOT Panchromatic and the synthesized 15 m Landsat TM image using ARSIS with a 2/3 filter bank. This approach is schematized in Figure 5. Note that the 15 m SPOT Panchromatic image is generated by the 2/3 filter bank.
- ***ARSIS$_{1/3}$ #2:*** in this case, the 30 m Landsat TM image is enhanced to 20 m by the use of ARSIS with a 2/3 filter bank and the SPOT Panchromatic resampled to a resolution of 20 m. Then the 10 m TM-HR image is synthesized from the 10 m SPOT Panchromatic and the synthesized 20 m Landsat TM image using ARSIS with a dyadic wavelet transform.

This second way consists in using a bicubic interpolation in order to circumvent the fact that the ratio of resolutions (*i.e.* 10 m and 30 m) is not a power of two. There are also two possible approaches:

- ***ARSIS$_{1/3}$ #3:*** the 30 m Landsat TM image is enhanced to 20 m by the use of a bicubic interpolation with resampling rate 2/3. Then the 10 m TM-HR image is synthesized from the 10 m SPOT Panchromatic and the synthesized 20 m Landsat TM image through ARSIS with a dyadic wavelet transform. The ARSIS$_{1/3}$ #3 approach is illustrated in Figure 6.
- ***ARSIS$_{1/3}$ #4:*** the 30 m Landsat TM image is resampled using the 2/3 wavelet transform to generate a 40 m TM image. Then ARSIS with a dyadic wavelet transform is applied twice to synthesize the 10 m TM-HR.

For both latter approaches, a bicubic interpolation is used: the Landsat TM images are changed into new images having a pseudo spatial resolution of either 20 m (*ARSIS$_{1/3}$ #3*) or 40 m (*ARSIS$_{1/3}$ #4*). As a consequence, the merging between SPOT and Landsat is not as complete as *ARSIS$_{1/3}$ #1* or *ARSIS$_{1/3}$ #2* because there is no injection of structures from the SPOT image between 30 m and 20 m in the case of *ARSIS$_{1/3}$ #3* or because of a degradation of the Landsat TM image resolution before the merging in the case of *ARSIS$_{1/3}$ #4*.

One can already see that *ARSIS$_{1/3}$ #4* will provide poorer results than *ARSIS$_{1/3}$ #3* because of the degradation of the original information prior to merging. Hence this approach is not studied any further. The study also shows that *ARSIS$_{1/3}$ #2* gives poorer results than *ARSIS$_{1/3}$ #1*, and for the sake of clarity of the article, the *ARSIS$_{1/3}$ #2* approach is not discussed any longer.

6. QUALITY ASSESSMENT OF THE SYNTHESIZED IMAGES

These different approaches - *ARSIS$_{1/3}$ #1* and *ARSIS$_{1/3}$ #3* - generate two sets of synthetic enhanced multispectral images. The quality of these sets is assessed by the mean of the protocol established by Mangolini *et al*. (1995) and Wald *et al.* (1997). The SPOT Panchromatic and the Landsat TM multispectral images are resampled to a lower resolution of respectively 30 and 90 m. Then, the fusion approaches are applied to synthesize TM multispectral images at 30 m called hereafter TM_1^*, ..., TM_5^*. Figure 7 illustrates the protocol of the quality assessment of the different approaches. Additionally, another approach is used to compute such enhanced images: the bicubic interpolation whose resampling rate is equal to 3. In fact, this approach does not belong to a merging scheme. That is to say that, in this approach, there is no structure injection from the 30 m SPOT Panchromatic. This additional computation is meant to assess, by comparison, the relevance of the different ARSIS mergings for the different spectral bands. All those images are then compared visually as well as on a pixel basis to the original TM images.

The quality of the synthesized images is firstly analyzed by a visual inspection of the 30 m TM^* images and secondly by a visual comparison between the original image (see Figure 1 for TM_1) and the synthesized 30 m images (see Figure 8 for TM_1^*). The $TM_1^{*\#1}$ image is obviously less blurred than

the $TM_1^{*\#3}$ one. See, for example, the limits of the fields in the pond in the lower part of images (a) and (b) in Figure 8. In other words, *$ARSIS_{1/3}$ #1* approach provides a better visual enhancement than the *$ARSIS_{1/3}$ #3* approach. However, the $TM_1^{*\#1}$ image presents several "wave like" artifacts near radiometric discontinuities in the image. It is clearly visible in the upper left part of the image (a) in Figure 8 and less important in the image (b). Those "vibrations" are due to Gibbs effects. The greater the number of coefficients of the filters used for the decomposition, the more important and visible these effects. It is the reason why the ARSIS concept applied with the 2/3 filter bank generates more artifacts near discontinuities than the approaches using only dyadic transforms.

The protocol for quality assessment also makes use of quantities. The original and synthesized 30 m images are compared numerically by computing their difference (original minus synthesized images) and their correlation. Ideally, the synthesized 30 m image should be similar to the original image , so that the difference should be null and correlation coefficient sould be 1. Several quantities are used to describe the discrepancies, and are described further. The quality assessment can be applied to the entire scene, and also to selected sub-scenes, such as that depicted in Figure 9a. This sub-scene is mainly composed of brushwood and forest and is crossed by a river (l'Arc). This zone is not very homogeneous and is composed of very thin structures. For the sake of brevity, only the study of the spectral bands TM_1, TM_2 and TM_5 is discussed because they are representative of all the important phenomena that have to be commented. We also do not present all the quantities computed to assess the performance of each approach. Some statistical characteristics for this sub-region are given in Table 1. We notice that, according to the homogeneity coefficient and the entropy measure, the TM_5 image is less homogeneous than the two others.

Figure 9 represents respectively the original sub-image TM1 and the different synthesized images: $TM_1^{*\#1}$, $TM_1^{*\#1}$ and $TM_1^{*\#BICUBIC}$. First we notice that the products of the different merging processes and the bicubic interpolation are blurred compared with the original image. See for instance the Arc river (upper left corner, in black). Nevertheless, the fusion approaches provide a better enhancement of the resolution than the bicubic interpolation even if differences between $TM_1^{*\#3}$ and $TM_1^{*\#BICUBIC}$ are small. This corroborates the fact that the merging introduces relevant structures in

the 90 m Landsat TM image while interpolation does not. Moreover, *ARSIS$_{1/3}$ #1* provides better results (less blurred) than *ARSIS$_{1/3}$ #3*: indeed, the first approach enables a better use of the structural information contained in SPOT Panchromatic than the latter one that calls partly upon interpolation (no structure introduced).

In Table 2 to 4 are given the different quantities used to describe the discrepanciesbetween the original and synthesized images:

- *The bias* is the mean of the difference between the synthesized and the original image. The second value is the relative bias *i.e.* the ratio between the bias and the mean of the original value. The closer the value to 0, the more similar the two images.
- *The difference of variances* (variance of the original image minus the variance of the synthesized image) and its relative value to the variance of the original image. This value is a measure, to some extent, of the quantity of information added or lost during the enhancement of the resolution. For an approach that provides too much information (information may be noise or artifacts) the difference is negative. In the opposite case, this value is positive. Ideally, this difference should be null.
- *The coefficient of correlation* between the original and the synthesized images shows the similarity between those images. It should be as close to 1 as possible.
- *The standard deviation of the difference*, and its relative value to the mean of the original image, globally indicates the level of pixel error. Ideally, they should be null.

This statistical comparison written on the above tables conjures up some comments. In the first place, it is observable that, owing to difference of variances, the bicubic interpolation approach suffers from a lack of information injection (about 15 %). This fact was foreseeable: indeed, this approach does not belong to a merging process and is in fact a resampling, *i.e.* a reorganization of the information from the 90 m TM images. But for the TM_5 channel, a similar observation is made for the *ARSIS$_{1/3}$ #3* approach. There is a lake of information injection between 2% and 5 %. This approach makes use of both bicubic interpolation to fill the gap between 60 m and 90 m and information from higher resolution (from 30 m and 60 m) of the degraded 60 m SPOT Panchromatic image. Hence the lack of

information can be partially explained by the fact that there is no injection of structure between 60 m and 90 m. On the other hand, the *ARSIS$_{1/3}$ #1* approach notably increases the amount of information (about 25 %). This increase of the variance which may prtly be due to noise is, to some extent, due to Gibbs effects.

In the second place, the *ARSIS$_{1/3}$ #1* approach provides better results for bias, standard deviation and correlation coefficient criteria for the spectral channels TM_1, TM_2 and TM_3. For the spectral bands TM_4 and TM_5, the best approach is obviously *ARSIS$_{1/3}$ #3*. This behavior of *ARSIS$_{1/3}$ #1* can partly be explained by the fact that the spatial structures in the first three channels are more correlated with those from Spot Panchromatic than TM_4 and TM_5 (see the correlation coefficients given in the second column of Table 5). In other words, this lack of correlation between the Panchromatic image and the TM_4 and TM_5 spectral bands decreases the quality of the result of the approach that obviously needs a sufficient level of spatial correlation. In addition, we see in Table 1 that the TM_5 channel (and also the TM_4 image) is less homogeneous than the TM_1 and TM_2. It follows that the Gibbs effect which degrades the quality of the *ARSIS$_{1/3}$ #1* is more likely important for the two last spectral bands.

Finally, Table 5 gives the correlation coefficient for the different spectral bands and for the original and the synthesized images. This table enables one to measure the increase of the dependence of the synthesized images upon the SPOT Panchromatic image and the inter-dependence between the synthesized images. As a whole, the merging approaches preserves the correlation coefficient within the data set. *ARSIS$_{1/3}$ #1* increases the dependence of the synthesized images upon the SPOT image as well as upon the spectral band TM_5. This is due to a too large injection of structures from the Panchromatic image into the TM^* images. The approach *ARSIS$_{1/3}$ #3* better preserves the correlation coefficient but at the expense of too much blurred images: in this case, not enough structures have been injected. Finally, the bicubic approach offers the worst preservation of the correlation coefficient because no structure at all is injected. However, for the same reason, it preserves fairly well the correlation between the TM spectral bands.

7. DISCUSSION

The quality of the ARSIS merging of Landsat TM multispectral with SPOT Panchromatic reveals less satisfactory then the quality obtained in the case of SPOT XS and Panchromatic images (e.g. Mangolini *et al.* 1995). This is true for visual and quantitative aspects, with and without the use of 2/3 filter bank Before drawing conclusions on the relevance of the use of rational filter banks within ARSIS concept, we examine the different reasons that could explain, regardless of those filters, the fairly bad results of the Landsat TM and SPOT Panchromatic merging.

Firstly, this could be explained partly by the fact that the images to merge are not perfectly co-registered and thus are not perfectly superimposable. But if we consider the case of SPOT XS and Panchromatic merging, very good results were attained even if those images are not perfectly co-registered. Hence these registration errors only degrade locally the quality of the merging, provided they are kept small. They do not explain the overall bad result.

Secondly, we could explain the bad results by the fact that the spectral redundancy between XS_1, XS_2, XS_3 and Panchromatic is more important than between some channels of Landsat TM and SPOT Panchromatic. But the merging of TM_6 (around 11.5 μm) and TM_7 (around 2.2 μm) described in Mangolini *et al.* (1992) provides results almost similar to the SPOT XS and Panchromatic merging. Thus it proves that the quality of ARSIS merging is nearly independent of the spectral characteristics of the images to merge and, in fact, depends on their local structure correlation. Therefore this lack of structure correlation only leads to local degradation of the quality and still does not explain the bad results.

The same comment applies when considering the time gap of the images to merge: in Mangolini *et al.* (1995) and Ranchin, Wald (1996), it is shown that the ARSIS merging is nearly independent of the time gap because it generally leads to very local and scarce differences.

From the discussion and regardless of the influence of the rational filter bank, two main explanations arise for these bad results:

- on the one hand, the larger resolution gap between the images to merge: in our case, the ratio of the resolution is 1/3 whereas, in the case SPOT XS and Panchromatic, the ratio is ½ ;
- on the other hand, the fairly bad quality of the Landsat images that are more noisy than the SPOT XS images.

The study shows that, even if the *ARSIS$_{1/3}$ #1* approach using the 2/3 filter bank can provide, under some conditions, better results than the other approaches, the quality of the merging is seriously degraded by some artifacts that cannot be entirely explained by the above reasons. These degradations seem to be mostly due to the use of the rational filter bank and raise serious doubts about its efficient application within ARSIS concept. Furthermore, it is maybe too sophisticated to be used in an operational and effective way relative to the benefits attained. We conclude that other ways to generalize the application of the ARSIS concept have to be invented.

The rational filter banks lie within the scope of the research into non-dyadic wavelet transforms like the work of Feauveau on $\sqrt{2}$ wavelet transform (Feauveau 1990). Indeed, they could be useful in other applications in satellite image processing such as structure analysis, because they can provide a large selection of multiresolution analyses that are sharper than dyadic wavelet transform.

8. ACKNOWLEDGMENT

The authors wish to thank Thierry Blu, from the CNET (France Telecom), for helpful technical and theorical advices as far as discrete rational wavelet transforms and rational filter banks synthesis are concerned. Philippe Blanc has a fellowship from the Ministry of Defense (DGA-DRET).

9. REFERENCES

BLU T., 1993-a, Iterated filter banks with rational rate changes. Connection with discrete wavelet transforms. *IEEE Transactions on Signal Processing*, 41, 3232-3244.

BLU T., 1993-b, Lossless filter design in two-band rational filter banks: a new algorithm. *In* Comptes-rendus du Quatorzième colloque GRETSI, Juan-Les-Pins, France, 69-72.

FEAUVEAU J.C., 1990, Analyse multirésolution pour les images avec un facteur de résolution $\sqrt{2}$.*Traitement du Signal*, vol. 7, 117-128.

MALLAT S.G., 1989, A theory for multiresolution signal decomposition: the wavelet representation. *IEEE Transactions on Pattern Analysis and Machine Intelligence*, 11, 674-693.

MANGOLINI M., RANCHIN T. and WALD L., 1992, Procédé et dispositif pour augmenter la résolution spatiale d'images à partir d'autres images de meilleure résolution spatiale. French patent n° 92-13691, November 20, 1992.

MANGOLINI M., RANCHIN T. and WALD L., 1993, Fusion d'images SPOT multispectrales (XS) et panchromatic (P), et d'images radar. *De l'optique au radar, les applications de SPOT et ERS*, p. 199-209, Cepaduès-Edition, 111 rue Vauquelin, Toulouse, France, 574 p.

MANGOLINI M., RANCHIN T. and WALD L., 1995, Evaluation de la qualité des images multispectrales à haute résolution spatiale dérivées de SPOT. *Bulletin de la Société Française de Photogrammétrie et Télédétection*, **137**, 24-29.

RANCHIN T. and WALD L., 1993, The wavelet transform for the analysis of remotely sensed images. *International Journal of Remote Sensing*, **14**, 135-159.

RANCHIN T., WALD L. and MANGOLINI M., 1993, Application de la transformée en ondelettes à la simulation d'images SPOT multispectrales de résolution 10 m *In* Comptes-rendus du Quatorzième colloque GRETSI, Juan-Les-Pins, France, 1387-1390.

RANCHIN T. and WALD L., 1996, Benefits of fusion of high spatial and spectral resolutions images for urban mapping. *In* Proceedings of the 26th International Symposium on Remote sensing of Environment and the 18th Annual Symposium of the Canadian Remote Sensing Society, Vancouver, British Columbia, Canada, March 25-29, 1996, p. 262-265.

WALD L., RANCHIN T. and MANGOLINI M., 1997, Fusion of satellite images of different spatial resolutions: assessing the quality of resulting images. *Photogrammetric Engineering & Remote Sensing*, 63, 691-699.

TABLE CAPTIONS

Table 1: means, variances, standard deviations, homogeneity coefficient (ratio in percent between standard deviation and mean) and entropy in radiance ($W \cdot m^{-2} \cdot sr^{-1} \cdot \mu m^{-1}$) of the sub-region of the original images for the spectral bands TM_1, TM_2 and TM_5.

Table 2: statistical criteria (bias, difference of variances, correlation coefficient and standard deviation of the difference) for comparison between TM_1 and TM_1* for the different approaches.

Table 3: statistical criteria (bias, difference of variances, correlation coefficient and standard deviation of the difference) for comparison between TM_2 and TM_2* for the different approaches.

Table 4: statistical criteria (bias, difference of variances, correlation coefficient and standard deviation of the difference) for comparison between TM_5 and TM_5* for the different approaches.

Table 5: correlation coefficient between the different spectral bands for the original Landsat multispectral, the SPOT Panchromatic and the different synthesized sub-images.

FIGURE CAPTIONS

Figure 1: original Landsat TM_1 (region of Berre l'Etang close to Marseille, France).

Figure 2: the different spectral bands of Landsat TM_1, ..., TM_5 images and SPOT Panchromatic.

Figure 3: general scheme of iterated rational filter banks.

Figure 4: one iteration of the 2/3 wavelet transform. (WT means wavelet transform).

Figure 5: illustration of the different stages of the approach $ARSIS_{1/3}$ #1.

Figure 6: illustration of the different stages of the approach $ARSIS_{1/3}$ #3.

Figure 7: Scheme of the protocol used to compare quantitatively and visually the quality of the different approaches.

Figure 8: (a) 30 m $TM_1^{*\#1}$ ($ARSIS_{1/3}$ #1*)*. (b) 30 m $TM_1^{*\#3}$ ($ARSIS_{1/3}$ #3*)*.

Figure 9: (a) Sub-region of the original Landsat TM (band TM_1). (b) Sub-region of $TM_1^{*\#1}$. (c) Sub-region of $TM_1^{*\#3}$. (d) Sub-region of $TM_1^{*\mathrm{BICUBIC}}$ (synthesized by bicubic interpolation).

	TM_1	TM_2	TM_5
Mean	3.42	4.10	2.71
Variance	0.25	0.82	0.65
Standard Deviation	0.5	0.9	0.80
Homogeneity Coefficient (Standard deviation / Mean)	15 %	22 %	30 %
Entropy	3.8	3.5	4.7

Table 6: means, variances, standard deviations, homogeneity coefficient (ratio in percent between standard deviation and mean) and entropy in radiance ($W \cdot m^{-2} \cdot sr^{-1} \cdot \mu m^{-1}$) of the sub-region of the original images for the spectral bands TM_1, TM_2 and TM_5.

		Bias (ideal: 0)	Variance of TM_1-variance of TM_1^* (ideal: 0)	Correlation coefficient (ideal: 1)	Standard deviation of the difference (ideal: 0)
TM_1	*$ARSIS_{1/3}$ #1*	0.00 0.0 %	-0.07 -25 %	0.83	0.30 9 %
	$ARSIS_{1/3}$ #3	0.00 0.0 %	0.006 3 %	0.80	0.31 9 %
	BICUBIC	0.00 0.0 %	0.04 17 %	0.73	0.36 11 %

Table 7: statistical criteria (bias, difference of variances, correlation coefficient and standard deviation of the difference) for comparison between TM_1 and TM_1* for the different approaches.

		Bias (ideal: 0)	Variance of TM_2-variance of TM_2^* (ideal: 0)	Correlation coefficient (ideal: 1)	Standard deviation of the difference (ideal: 0)
TM_2	*$ARSIS_{1/3}$ #1*	0.00 0.0 %	-0.16 -20 %	0.85	0.53 13 %
	$ARSIS_{1/3}$ #3	0.00 0.1 %	0.03 4 %	0.80	0.56 14 %
	BICUBIC	0.00 0.1 %	0.14 17 %	0.73	0.64 16 %

Table 8: statistical criteria (bias, difference of variances, correlation coefficient and standard deviation of the difference) for comparison between TM_2 and TM_2* for the different approaches.

		Bias (ideal: 0)	Variance of TM_5-variance of TM_5^* (ideal: 0)	Correlation coefficient (ideal: 1)	Standard deviation of the difference (ideal: 0)
TM_5	*$ARSIS_{1/3}$ #1*	0.00 0.0 %	-0.22 -34 %	0.81	0.56 21 %
	$ARSIS_{1/3}$ #3	0.00 0.0 %	0.02 -3 %	0.82	0.48 18 %
	BICUBIC	0.00 0.0 %	0.08 12 %	0.77	0.53 20 %

Table 9: statistical criteria (bias, difference of variances, correlation coefficient and standard deviation of the difference) for comparison between TM_5 and TM_5* for the different approaches.

	ORIGINAL	*ARSIS$_{1/3}$ #1*	*ARSIS$_{1/3}$ #3*	*BICUBIC*
PAN-TM$_1$	0.752	0.815	0.691	0.589
PAN-TM$_2$	0.773	0.830	0.709	0.628
PAN-TM$_5$	0.665	0.769	0.658	0.547
TM$_1$-TM$_2$	0.966	0.968	0.966	0.969
TM$_1$-TM$_5$	0.765	0.817	0.786	0.790
TM$_2$-TM$_5$	0.809	0.841	0.825	0.833

Table 10: correlation coefficient between the different spectral bands for the original Landsat multispectral, the SPOT Panchromatic and the different synthesized sub-images.

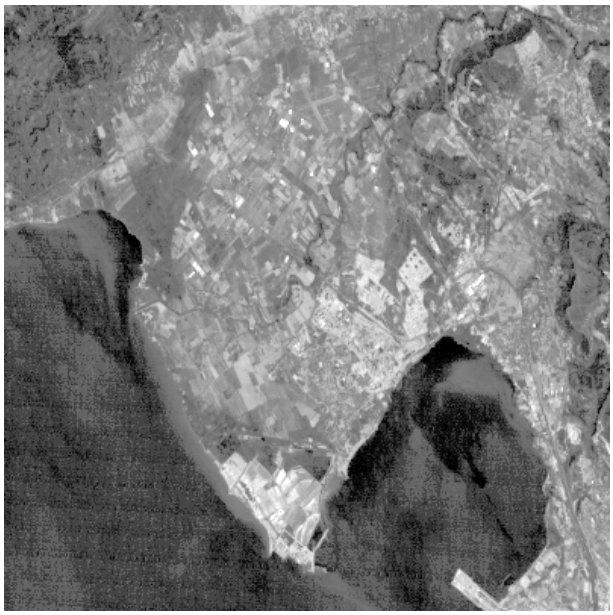

Figure 1: original Landsat TM_1 (region of Berre l'Etang close to Marseille, France).

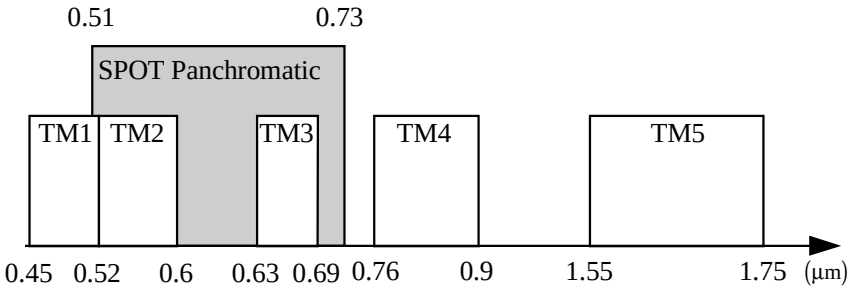

Figure 2: the different spectral bands of Landsat TM_1, ..., TM_5 images and SPOT Panchromatic.

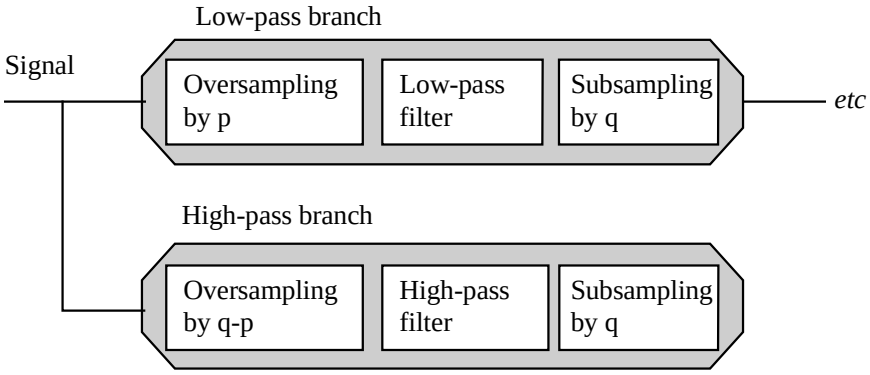

Figure 3: general scheme of iterated rational filter banks.

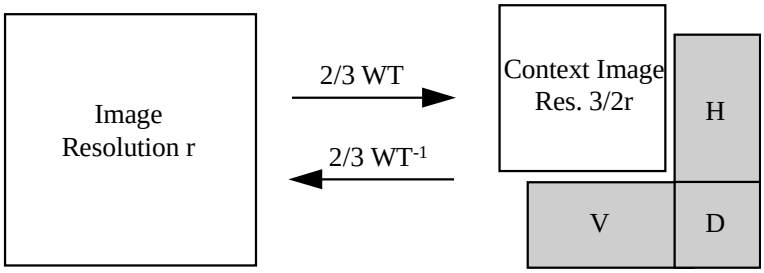

Figure 4: one iteration of the 2/3 wavelet transform. (WT means wavelet transform).

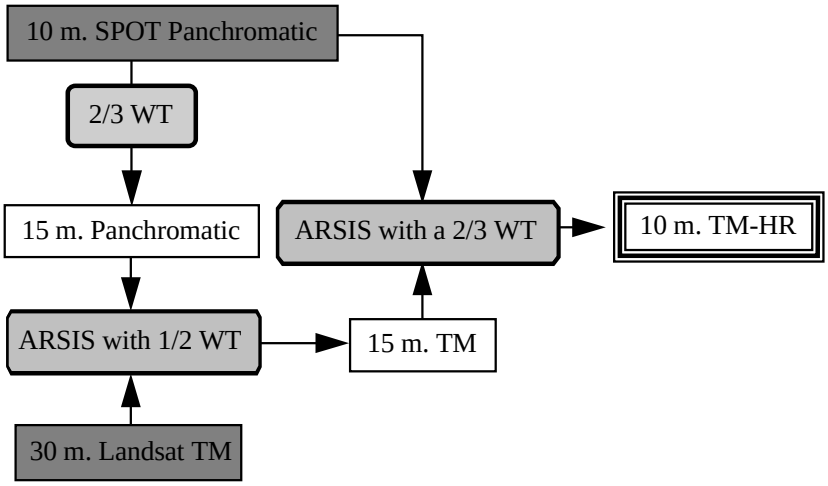

Figure 5: illustration of the different stages of the approach $ARSIS_{1/3}$ #1.

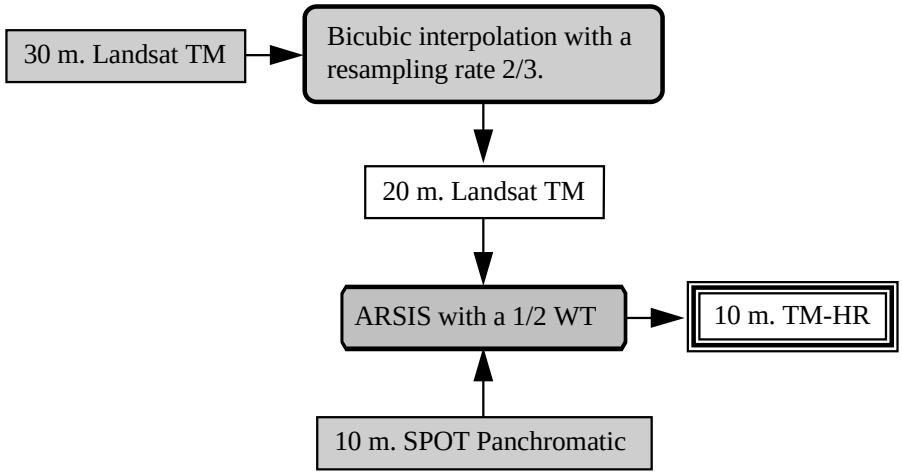

Figure 6: illustration of the different stages of the approach $ARSIS_{1/3}$ #3.

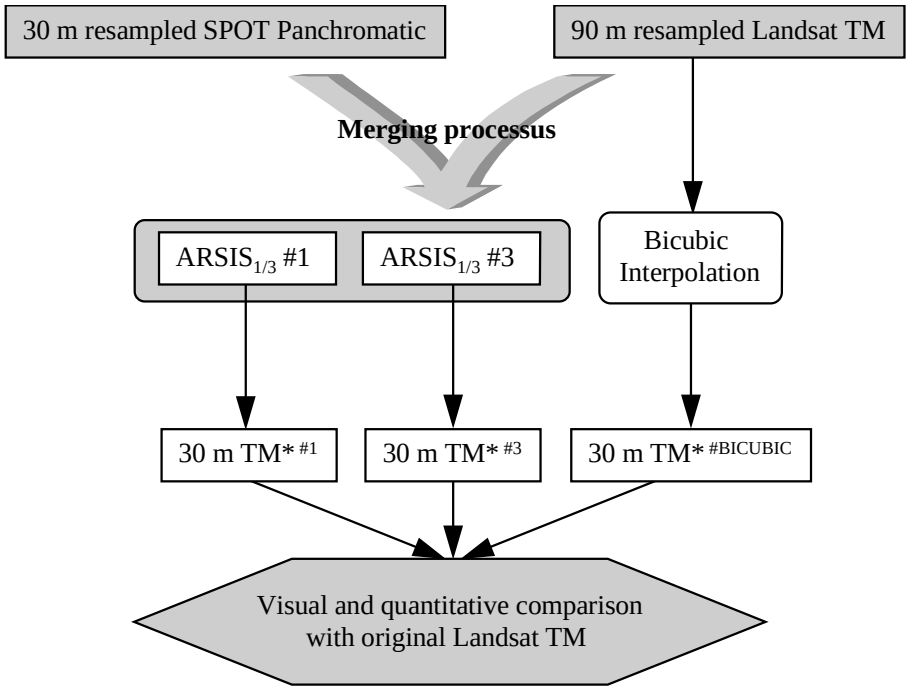

Figure 7: Scheme of the protocol used to compare quantitatively and visually the quality of the different approaches.

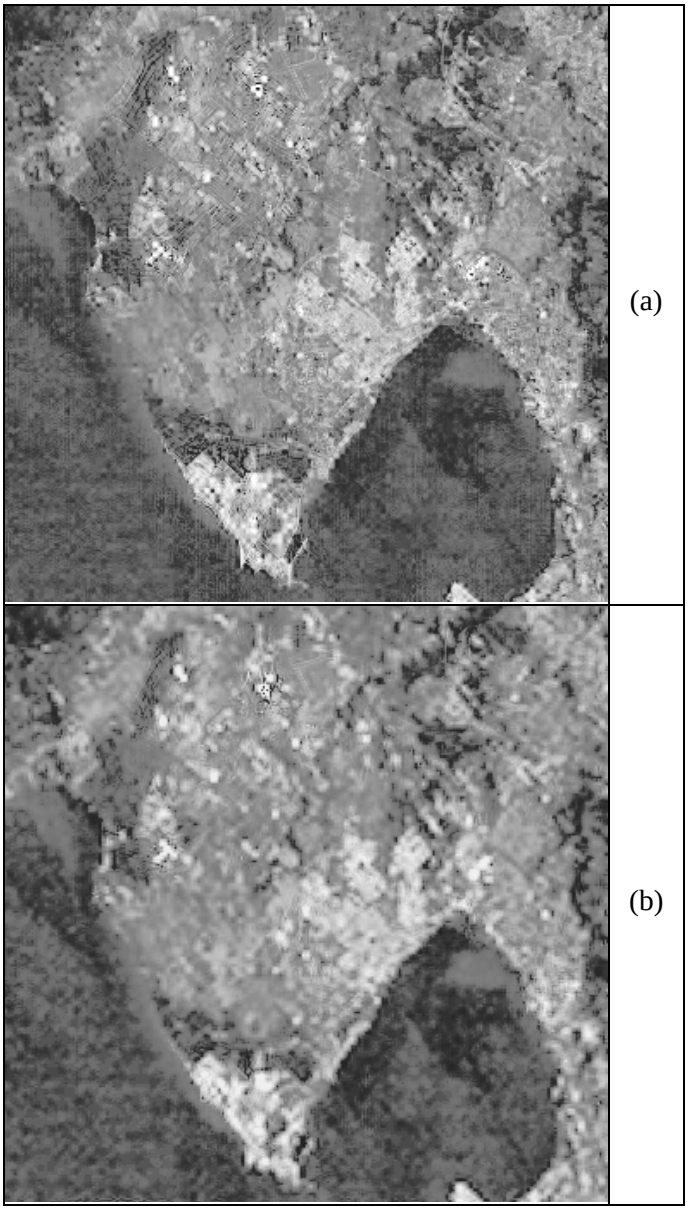

Figure 8: (a) 30 m $TM_1^{*\#1}$ ($ARSIS_{1/3}$ #1*)*. (b) 30 m $TM_1^{*\#3}$ ($ARSIS_{1/3}$ #3*)*.

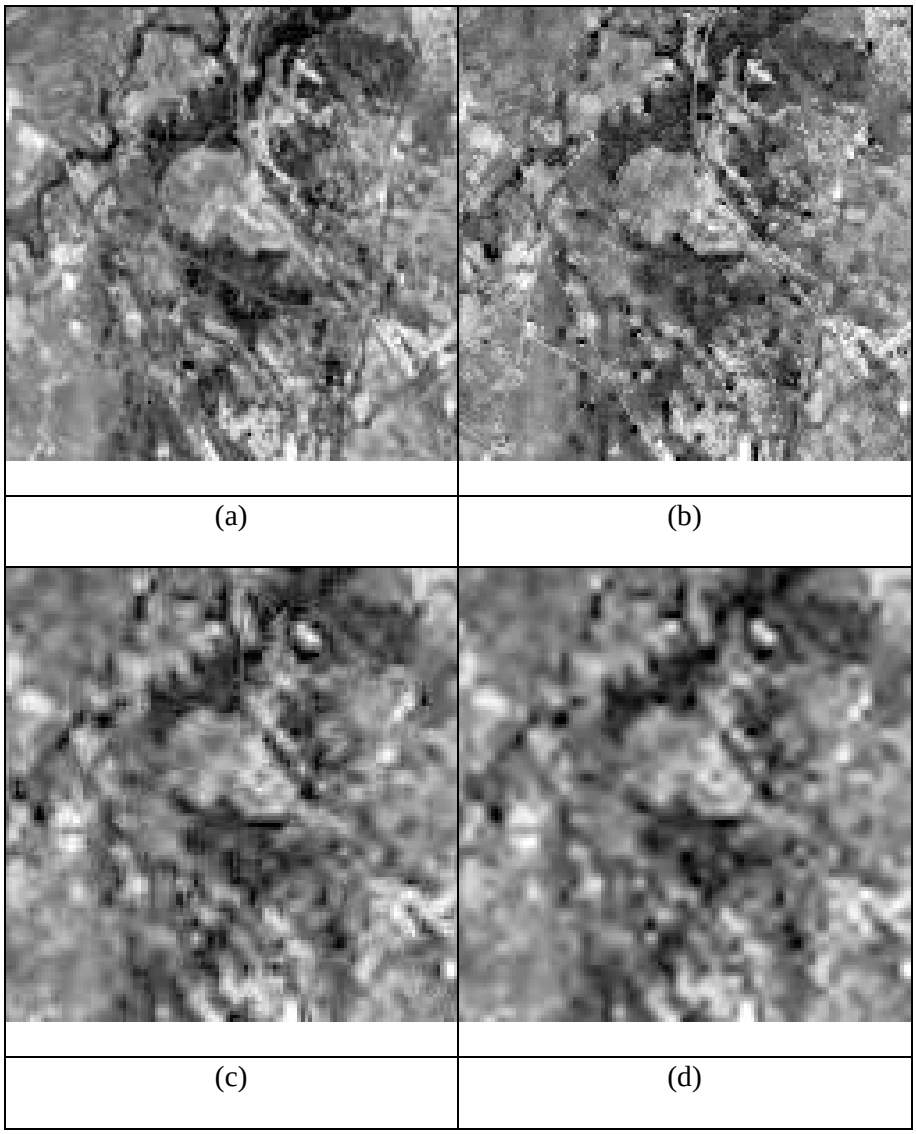

Figure 9: (a) Sub-region of the original Landsat TM (band TM_1). (b) Sub-region of $TM_1^{*\#1}$. (c) Sub-region of $TM_1^{*\#3}$. (d) Sub-region of $TM_1^{*BICUBIC}$ (synthesized by bicubic interpolation).